NUMERICAL INVESTIGATION OF LIFTED TURBULENT FLAME WITH PASR AND FPV MODELS

Z. Li [1,2,3]*, R. Mahmoud* [2]*, A. Sadiki* [2] *and A. Parente* [1,3]

[1] *Université Libre de Bruxelles, Ecole polytechnique de Bruxelles, Aero-Thermo-Mechanics Laboratory, Belgium*
[2] *Technische Universität Darmstadt, Institute of Energy and Powerplant technology, Germany*
[3] *Université Libre de Bruxelles and Vrije Universiteit Brussel, Combustion and Robust Optimization Group (BURN), Belgium*

Zhiyi.Li@ulb.ac.be

Abstract

The current study focuses on the Unsteady Reynolds Averaged Navier-Stokes (URANS) simulation of a lifted methane flame with vitiated co-flow. The combustion models of Partially Stirred Reactor (PaSR) and Flamelet Progress Variable (FPV) are adopted and compared. Three kinetic mechanisms (KEE58, GRI3.0 and San-Diego) with increasing number of species and reactions are used with PaSR model. Results have shown that using the San-Diego mechanism provides better simulation results regarding the mean temperature and species mass fraction, which reveals the importance of chemistry kinetics on the lifted flame. The PaSR model is able to predict the current flame with satisfaction. However, the FPV models shows its limitation on the case when transient phenomenon like extinction and re-ignition exist.

1 Introduction

In order to meet the objective of low-emission energy strategy, techniques such as the combustion of lean and diluted fuel-air mixture have been proposed [7]. To achieve the diluted condition, Exhaust Gas Recirculation (EGR) is often used in applicational combustion systems [5]. The mixing of the fresh gases and the hot products leads to auto-ignition of the flame and the temperature field is homogenized because of reduced reactivity. As a result, the amount of NO_x emission is highly reduced. Furthermore, the thermal energy contained in the hot products helps to stabilize the flame [24].

If the central jet has enough high velocity, the auto-ignited flame will be lifted. The lifted and diluted condition can lead to reduced Damköhler numbers, which indicates a strong multi-scale interaction between the chemistry kinetics and turbulent mixing [7]. Predicting such flames in industrial level with complex geometry is a great challenge to the turbulent and combustion models used. The Cabra [2] vitiated co-flow flame provides a simplification, by using a jet with simple geometry. Moreover, the co-flow area with large diameter isolates the contact of central fuel with ambient air for a long distance, avoiding complexities with three streams.

The stabilization of Cabra flame is a balance between chemical reactions and fluid dynamics [10]. Therefore, unlike mixing-controlled flames, models that exclude detailed kinetics are not able to capture the multi-scale process. The Partially Stirred Reactor (PaSR) [3] has been reported to handle the turbulence-chemistry interaction well, not only in conventional combustion regime [9, 11, 18, 19], but also under non-conventional condition, like MILD combustion[6]. In PaSR, the influence of the turbulence on the reaction rate is expressed with a factor κ, defined as the ratio between the characteristic chemical time scale and the sum of the chemical and mixing time scales. On the other hand, the flamelet-like models are one of the most commonly used models in turbulent combustion. The relation between turbulence and chemistry is described with several representative variables, and it requires low computational cost. In the present work, the Flamelet Progress Variable (PFV) model proposed by Pierce & Moin (2001, 2004) [13, 14] is chosen to compare with the PaSR model regarding their abilities on turbulence-chemistry interaction prediction.

The objective of the current article is to demonstrate the importance of chemistry kinetics in the diluted and lifted flame and to evaluate the performance of combustion models in multi-scale reacting flows. Two combustion models, the finite-chemistry based Partially Stirred Reactor (PaSR) model and the tabulated chemistry based Flamelet Progress Variable (PFV) model are validated against high fidelity experimental data from Cabra et al (2005) [2]. Three chemical mechanisms, the KEE58 [1], GRI3.0 [21] and San-Diego [22] are used. Finite Volume Method (FVM) based URANS (Unsteady Reynolds Averaged Navier-Stokes) simulation is applied on all the cases.

2 Methodology

PaSR model

In the PaSR model [3, 6], each computational cell is split into two zones: one where reactions take place, and another characterized by only mixing. The final

average species concentration of the cell is determined by the mass exchange between the two zones, driven by the turbulence. The mean chemical source term is formulated as:

$$\overline{\dot{\omega}}_i = \kappa \frac{\widetilde{\rho}\left(Y_i^* - Y_i^0\right)}{\tau^*}, \tag{1}$$

where τ^* represents the residence time in the reactive zone, Y_i^0 is the initial i_{th} species mass fraction in the non-reactive region and Y_i^* is the i_{th} species mass fraction in the reactive zone. The quantity κ is the mass fraction of the reaction zone in the computational cell, which is evaluated as [9]:

$$\kappa = \frac{\tau_c}{\tau_c + \tau_{mix}}, \tag{2}$$

where τ_c and τ_{mix} are the characteristic chemical and mixing time scale in each cell, respectively.

In order to get the value of Y_i^*, a time-splitting approach is applied. The reactive zone is modelled as an ideal reactor evolving from Y_i^0, during a residence time τ^*:

$$\frac{dY_i^*}{dt} = \frac{\dot{\omega}_i}{\rho}. \tag{3}$$

The term $\dot{\omega}_i$ is the instantaneous formation rate of species i. The final integration of $\frac{dY_i^*}{dt}$ over the residence time τ^* in the reactor is Y_i^*. The characteristic of PaSR model lies in the fact that the Ordinary Differential Equations (ODEs) of the reactions and the transport equations of scalar quantities are solved to obtain the composition space.

Dynamic estimation of mixing time scale. For the estimation of mixing time scale τ_{mix} in PaSR model, a dynamic approach which involves solving the transport equations are adopted. It is based on the ratio of the scalar variance, $\widetilde{\phi''^2}$, to the scalar dissipation rate, $\widetilde{\epsilon_\phi}$ [17]:

$$\tau_{mix} = \frac{\widetilde{\phi''^2}}{\widetilde{\epsilon_\phi}}. \tag{4}$$

The mixture fraction Z is selected to describe the mixing process. Therefore, the mixture fraction variance ($\widetilde{Z''^2}$) and mixture fraction dissipation rate ($\widetilde{\chi}$) are used. They are obtained from solving the transport equations[23, 20]. In the transport equations, there are four constants used: C_1, C_2, C_3 and C_4. Different combination of values are available in the literature [23, 20]. In the present article, the second set (C_1 = 1.0, C_2 = 1.8, C_3 = 3.4 and C_4 = 1.4) and third set (C_1 = 2.0, C_2 = 1.8, C_3 = 3.4 and C_4 = 1.4) from Ye et al (2011) is used. They are referred to as dyn2 and dyn3, respectively.

Chemical time scale estimation from formation rates. For the evaluation of chemical time scale, the ratio of species mass fraction and formation rate in the reactive zone is used [4]:

$$\tau_{c,i} = \frac{Y_i^*}{|dY_i^*/dt|}. \tag{5}$$

In Eqn. 5, $\tau_{c,i}$ is the characteristic time scale of a single species; after removing the dormant species (characterised by infinite time scale values), the slowest chemical time scale is chosen as leading scale for the evaluation of the PaSR parameter κ.

FPV model

Based on the assumption of the flamelet model [12], which considers a turbulent diffusion flame as an ensemble of laminar flamelets, the FPV model obtains the composition space from solving scalar transport equations of mixture fraction Z and progress variable C [14]:

$$\frac{\partial \bar{\rho}\widetilde{Z}}{\partial t} + \nabla \cdot \bar{\rho}\widetilde{\mathbf{u}}\widetilde{Z} = \nabla \cdot \left[\bar{\rho}(\widetilde{D}_Z + D_t)\nabla \widetilde{Z}\right], \tag{6}$$

$$\frac{\partial \bar{\rho}\widetilde{C}}{\partial t} + \nabla \cdot \bar{\rho}\widetilde{\mathbf{u}}\widetilde{C} = \nabla \cdot \left[\bar{\rho}(\widetilde{D}_C + D_t)\nabla \widetilde{C}\right] + \bar{\rho}\widetilde{\omega}_C, \tag{7}$$

where D_t is the turbulent diffusivity and the$\widetilde{}$ denotes the favre averaged values. The favre averaged specie mass fraction $\widetilde{y}_i$ and chemical source term $\widetilde{\omega}_C$ are calculated by integrating laminar composition state from flamelet library over the joint PDF of Z and C:

$$\widetilde{y}_i = \int y_i\left(Z, C\right) \widetilde{P}\left(Z, C\right) dZdC, \tag{8}$$

$$\widetilde{\omega}_C = \int \omega_C\left(Z, C\right) \widetilde{P}\left(Z, C\right) dZdC. \tag{9}$$

The joint PDF $\widetilde{P}\left(Z, C\right)$ is modelled by:

$$\widetilde{P}\left(Z, C\right) = \widetilde{P}\left(C|Z\right) \widetilde{P}\left(Z\right), \tag{10}$$

where $\widetilde{P}\left(Z\right)$ is described by a beta PDF and $\widetilde{P}\left(C|Z\right)$ is determined by a delta function:

$$\widetilde{P}\left(C|Z\right) = \delta(C - \widetilde{C|Z}). \tag{11}$$

The definition of Progress Variable (PV) C is defined using the mass fraction of CO, CO_2 and H_2O in the current work.

3 Experimental and numerical details

The lifted flame with vitiated co-flow [2] has a central jet with the inner diameter of d = 4.57 mm, containing a mixture of 33 % CH_4 and 67 % air by volume. A coaxial flow with hot combustion products from a lean H_2-air flame is provided. The bulk velocity of the fuel and co-flow are 100 m/s and 5.4 m/s, receptively, and the co-flow mean temperature is 1350 K. A 2D schematic drawing of the Cabra lifted flame can be seen in Figure 1

An axi-symmetric 2D structured mesh containing 30840 cells is used for URANS simulation. It extends

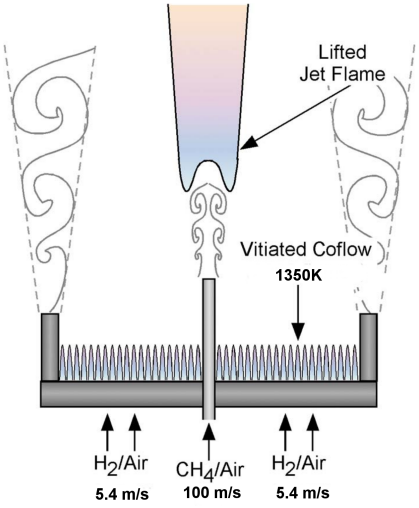

Figure 1: 2D schematic drawing of Cabra lifted flame (adapted from Cabra et al. [2]).

70 d downstream of the fuel nozzle exit and 20 d radially. Pre-inlet pipe is constructed for the fuel jet, which is discretized with 12 cells. The standard k-ϵ model is adopted as turbulence model. The KEE58 (17 species, 58 reactions) [1], GRI3.0 (53 species, 325 reactions) [21] and San-Diego(50 species, 247 reactions) [22] kinetic mechanisms with increasing complexity are chosen for detailed chemistry approach. The sampling locations are z/d (z is the axial direction) = 15, 30, 40, 50 70 and the centerline.

4 Results and discussion

The influence of chemical kinetics

In this section, the PaSR model with dyn2 constants is used for simulation with three different kinetic mechanisms. The mean temperature profiles on the sampling locations are compared to the experimental measurement data in Figure 2. The radial (z/d = 15, 30, 40, 50 and 70) mean temperature profiles shows that the flame is not ignited when KEE58 mechanism is used. A slight increase of temperature can be captured with GRI3.0. However, there is a huge underprediction of temperature compared to the experimental value. When it comes to the San-Diego mechanism, though early ignition is observed on z/d = 30, the flame is fully ignited. This is especially obvious when looking at the centerline value.

The influence of flame ignition can be revealed from the flow field properties as well. Figure 3 shows the mixture fraction distribution from the cases using the three different mechanisms. Similar profiles are shown for z/d $\leq$ 40. Obvious discrepancies are captured on z/d = 70 and z $\geq$ 250 mm, with using San-Diego mechanism provides closer results to the measured profiles.

The heat release rate contour plot in Figure 4 provides more visual look on the flame ignition. From

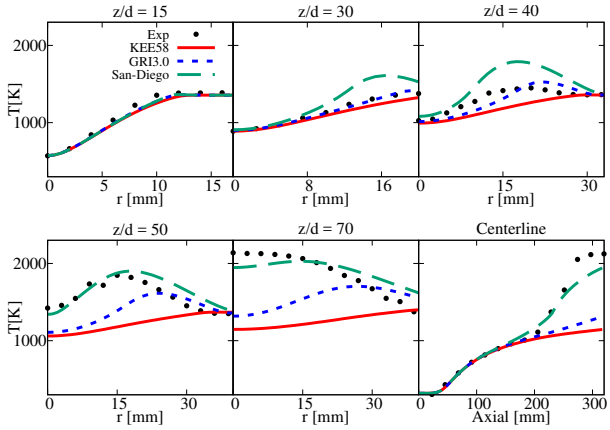

Figure 2: Mean temperature profiles on z/d = 15, 30, 40, 50, 70 and the centerline with three different mechanisms (KEE58, GRI3.0 and San-Diego) in creasing complexity.

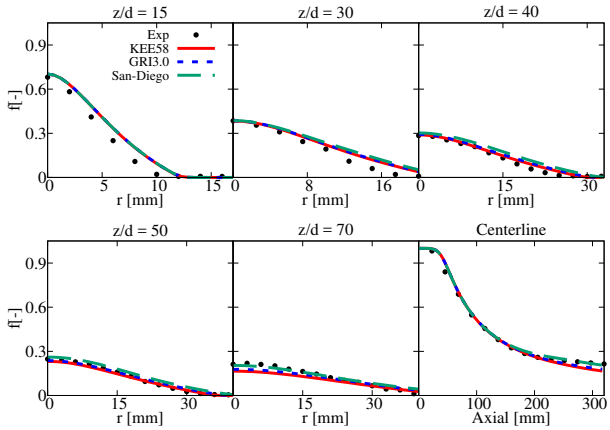

Figure 3: Mean mixture fraction profiles on z/d = 15, 30, 40, 50, 70 and the centerline with three different mechanisms (KEE58, GRI3.0 and San-Diego) in creasing complexity.

KEE58 to San-Diego (from left to right), the heat release happens earlier and the absolute amount is increased as well. Furthermore, heat release is captured close to the centerline downstream of the jet (z $\geq$ 220 mm) only when San-Diego mechanism is used.

Comparison of PaSR and FPV models

The dyn3 constants are used in this section in order to increase the accuracy of prediction with PaSR model. The San-Diego mechanism is chosen and the other numerical properties are kept the same except combustion model adopted. The FlameMaster [15] toolkit is used and 1D diffusion steady flamelets are generated to construct the lookup-table for FPV model. The S curve obtained by plotting the maximum temperature of each flamelet versus the scalar stoichiometric dissipation rate is presented in Figure 5. Since the temperature of co-flow is 1350 K, the lower branch of the non-burning solutions reaches a plateau at around 1350 K. The middle branch which represents unstable burning condition is also included in the cur-

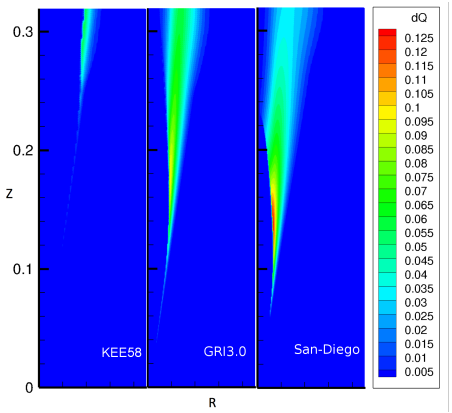

Figure 4: Contour plot of heat release rate (J/s) with three different mechanisms (KEE58, GRI3.0 and San-Diego) in creasing complexity. Unit: m.

rent calculation.

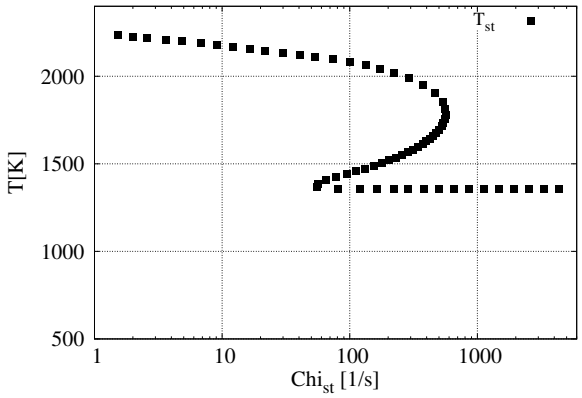

Figure 5: S curve obtained by plotting the maximum temperature of each flamelet versus the scalar stoichiometric dissipation rate.

Figure 6 shows the comparison of mean temperature profiles obtained from cases using PaSR and FPV models. It is obvious to see that the FPV model provides very early ignition, a sudden increase of temperature is observed at around z = 100 mm on the centerline. Upstream (z/d $\leq$ 50) temperature field is highly over-predicted. On the contrary, the PaSR model gives reasonable predictions for upstream region, although slight over-prediction is captured on z/d = 50. Further downstream, at z/d = 70 and after, FPV model shows its advantage by predicting mean temperature better than PaSR model.

The process of combustion process can be revealed by the oxidiser distribution as well. In Figure 7, when the FPV model is used, O_2 is rapidly consumed from around axial location of z = 80 mm, according to the centerline profile. While as with the PaSR model, in agreement with the experimental data, the sharp decrease of O_2 centerline value happens until z = 200 mm. Such trend can be observed for z/d = 15, 30, 40 and 50 as well. As with z/d = 70, similar to the

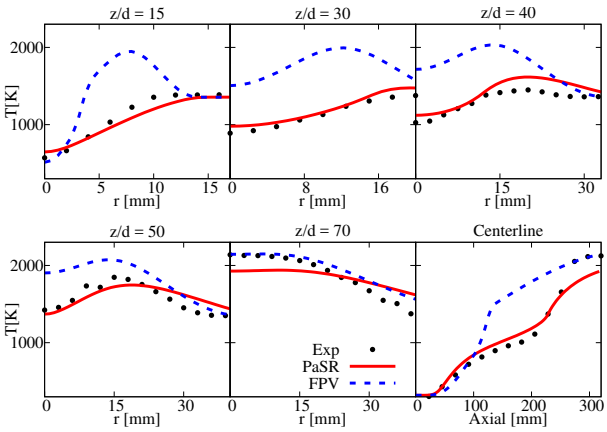

Figure 6: Mean temperature profiles on z/d = 15, 30, 40, 50, 70 and the centerline obtained from cases using PaSR anf FPV combustion models.

mean temperature profile, using FPV models provides better prediction. Using the PaSR model is not able to consume enough O_2 for z $\geq$ 250 mm, and this results in reduced production of CO_2 (not shown here) and H_2O (see Figure 8). On the other hand, the FPV models seems to be failed to handle the intense turbulence and chemistry interaction region (100 mm $\leq$ z $\leq$ 250 mm).

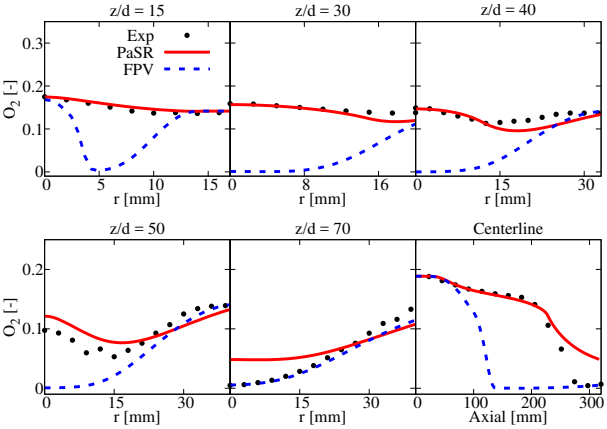

Figure 7: Mean O_2 mass fraction profiles on z/d = 15, 30, 40, 50, 70 and the centerline obtained from cases using PaSR anf FPV combustion models.

In Figure 8, the PaSR model predicts the mean H_2O with good agreement to the experimental data on most sampled locations, except on the centerline direction from z = 250 mm downward. The FPV model still shows obvious over-prediction, especially upstream.

The choice of combustion model has influence on flow field as well. Satisfactory agreement with the experimentally measured value is found for mean mixture fraction using the PaSR model. When it comes to the FPV model, much slower jet decay is presented and the only well predicted location locates at z/d = 70, as it is with T and O_2.

The OH distribution from the cases with PaSR and

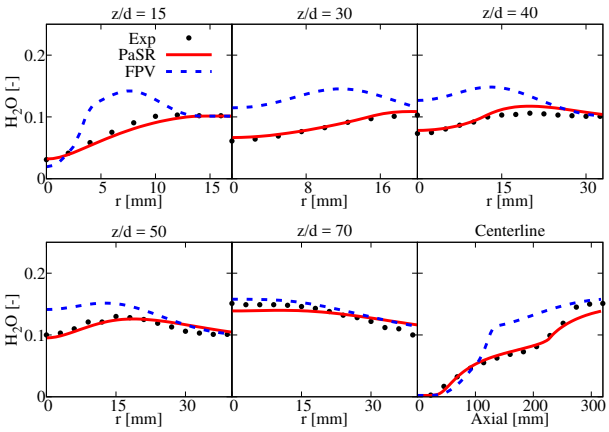

Figure 8: Mean H_2O mass fraction profiles on z/d = 15, 30, 40, 50, 70 and the centerline obtained from cases using PaSR anf FPV combustion models.

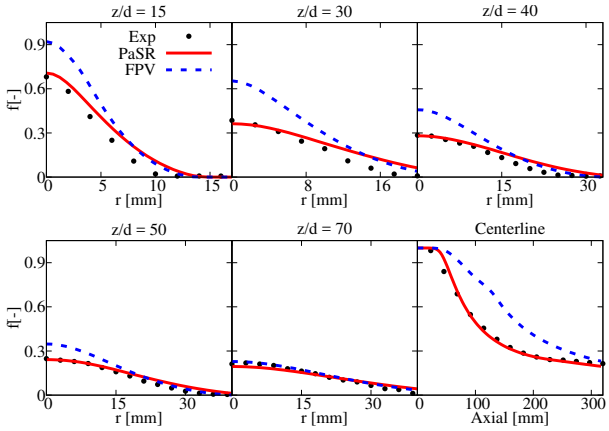

Figure 9: Mean mixture fraction profiles on z/d = 15, 30, 40, 50, 70 and the centerline obtained from cases using PaSR anf FPV combustion models.

FPV model is shown in Figure 10. The flame is lifted to around 100 mm when PaSR model is used. Such flame lift off height corresponds to around 22 d, which is lower than the experimental measured height, 35 d. Regarding the case with FPV model, the flame is ignited almost immediately at the jet outlet location, showing no lift-off of the flame.

The lifted flame is caused by the high velocity, indicating the existence of flame extinction between the length from jet outlet to flame stabilization location. Since PaSR models the reactive region in each cell by solving the Ordinary Differential Equations (ODEs) of the reactions and τ_{mix} is included explicitly in the calculation of κ, the interaction of chemistry and turbulence is updated for each time step. However, the FPV model reads the lookup-table which is obtained from steady diffusion flame. Unsteady situations (flame extinction and re-ignition) can not be fully covered with the generated table.

5 Conclusions

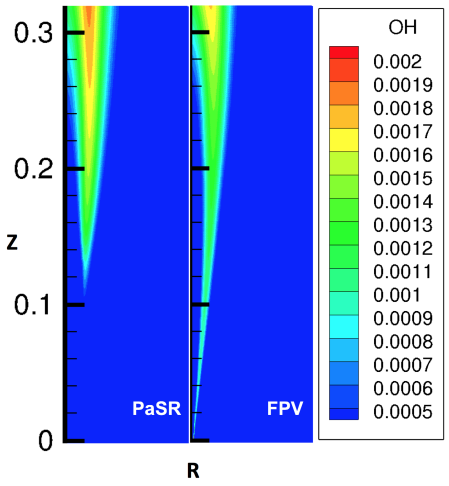

Figure 10: Contour plot of OH mass fraction obatined from cases with PaSR and FPV models. Unit: m.

The present article compares three different mechanism with increasing complexity with Partially Stirred Reactor (PaSR) model. The performance of PaSR and Flamelet Progress Variable (FPV) model are evaluated regarding their predictions on mean temperature, species mass fraction and mixture fraction of the Cabra flame. The conclusion can be summarized as:

- The Cabra methane flame is very sensitive to the chemistry kinetics used because of the strong interaction between chemistry and turbulence. Therefore detailed mechanism is required for simulating such flame.
- The case with PaSR model provides overall better predicted profiles than that with FPV model. The FPV model fails to handle the complex multi-scale situation.
- Neither of the models give correct flame lift-off height, indicating further work on the turbulence model and properties used.
- Even though full S-curve is included in the flamelet table, the current steady FPV model does not predict the lifted flame well. The generated flamelets come from a steady solution; however, extinction and reignition phenomena driven by turbulence create transient states which are away from the steady solutions. Therefore, the steady FPV model shows limited performance on flames with strong turbulence-chemistry interaction. For the prospectives, the Unsteady Flamelet Progress Variable (UFPV) [16, 7] is expected to be used on the current flame. A new definition of Progress Variable (PV) using Principle Component Analysis (PCA) [8] is planned to be implemented as well.

Acknowledgments

This project has received funding from the European Union′s Horizon 2020 research and innovation program under the Marie Skłodowska-Curie grant agreement No. 643134. The research of the last author is sponsored by the European Research Council, Starting Grant No. 714605.

6 *

References

[1] Bilger, R. W., Stårner, S. H., and KEE, R. J. (1990). On reduced mechanisms for methane-air combustion in nonpremixed flames. *Combustion and Flame*, 80(2):135–149.

[2] Cabra, R., J.-Y.Chen, Dibble, R., A.N.Karpetis, and Barlow, R. (2005). Lifted methane-air jet flames in a vitiated coflow. *Combustion and Flame*, 143:491–506.

[3] Chomiak, J. (1990). *Combustion: a study in theory, fact and application*. Abacus press/gorden and breach science publishers.

[4] Chomiak, J. and Karlsson, A. (1996). Flame liftoff in diesel sprays. In *Twenty-Sixth Symposium (International) on Combustion*, pages 2557–2564. The Combustion Institute.

[5] Domingo, P., Vervisch, L., and Veynante, D. (2008). Large-eddy simulation of a lifted methane jet flame in a vitiated coflow. *Combustion and Flame*, 152(3):415–432.

[6] Golovitchev, V. and Chomiak, J. (2001). Numerical modelling of high temperature air "flameless" combustion. In *the 4th international symposium on high temperature air combustion and gasification*, Rome, Italy. the 4.

[7] Ihme, M. and See, Y. C. (2010). Prediction of autoignition in a lifted methane/air flame using an unsteady flamelet/progress variable mode. *Combustion and Flame*, 157:1850–1862.

[8] Jolliffe, I. T. (2002). *Principal component analysis*. Springer, New York, NY.

[9] Kärrholm, F. P. (2008). *Numerical modelling of diesel spray injection, turbulence interaction and combustion*. PhD thesis, Chalmers University of Technology.

[10] Navarro-Martinez, S. and Kronenburg, A. (2009). Les-cmc simulations of a lifted methane flame. *Proceedings of the Combustion Institute*, 32(1):1509–1516.

[11] Nordin, P. A. N. (2001). *Complex chmisrey modeling of diesel sparay combustion*. PhD thesis, Chalmers University of Technology.

[12] Peters, N. (1984). Laminar diffusion flamelet models in non-premixed turbulent combustion. *Progress in Energy and Combustion Science*, 10:319–339.

[13] Pierce, C. D. and Moin, P. (2001). *Progress-Variable Approach for Large Eddy Simulation of Turbulent Combustion*. PhD thesis, Stanford University.

[14] Pierce, C. D. and Moin, P. (2004). Progress-variable approach for large eddy simulation of non-premixed turbulent combustion. *Journal of Fluid Mechanics*, 504:73–97.

[15] Pitsch, H. *FlameMaster, A C++ Computer Program for 0D Combustion and 1D Laminar Flame Calculations.*

[16] Pitsch, H. and Ihme, M. (2005). An unsteady/flamelet progress variable method for les of nonpremixed turbulent combustion. In *43rd AIAA Aerospace Sciences Meeting and Exhibit*, Reno, NV.

[17] Raman, V. and Pitsch, H. (2007). A consistent LES/filtered-density function formulation for the simulation of turbulent flames with detailed chemistry. *Proceedings of the Combustion Institute*, 31(2):1711– 1719.

[18] Sabelnikov, V. and Fureby, C. (2013a). Extended les-pasr model for simulation of turbulent combustion. *Progress in Propulsion Physics*, 4:539–568.

[19] Sabelnikov, V. and Fureby, C. (2013b). Les combustion modeling for high re flames using a multiphase analogy. *Combustion and Flame*, 160:83–96.

[20] Sanders, J. P. H. and Gökalp, I. (1998). Scalar dissipation rate modelling in variable density turbulent axisymmetric jets and diffusion flames. *Physics of Fluids*, 10(4):938–948.

[21] Smith, G. P., Golden, D. M., Frenklach, M., Moriarty, N. W., Eiteneer, B., Goldenberg, M., Bowman, C. T., Hanson, R. K., Song, S., Gardiner, W. C., Jr., Lissianski, V. V., and Qin, Z.

[22] University of California at San Diego. Chemical-kinetic mechanisms for combustion applications.

[23] Ye, I. (2011). *Investigation of the scalar variance and scalar dissipation rate in URANS and LES*. Phd thesis, University of Waterloo, Ontario, Canada, Waterloo, Ontario, Canada.

[24] Zhang, H., Yu, Z., Ye, T., Zhao, M., and Cheng, M. (2018). Large eddy simulation of turbulent lifted flame in a hot vitiated coflow using tabulated detailed chemistry. *Applied Thermal Engineering*, 128:1660–1672.